Published in final edited form as:

Nat Chem Biol. 2017 April ; 13(4): 366–368. doi:10.1038/nchembio.2285.

Structure and Specificity of a Permissive Bacterial *C*-Prenyltransferase

Sherif I. Elshahawi[1,2], **Hongnan Cao**[3], **Khaled A. Shaaban**[1,2], **Larissa V. Ponomareva**[1,2], **Thangaiah Subramanian**[4], **Mark L. Farman**[5], **H. Peter Spielmann**[4,6], **George N. Phillips Jr.**[3,*], **Jon S. Thorson**[1,2,*], and **Shanteri Singh**[2,7,*]

[1]Department of Pharmaceutical Sciences, College of Pharmacy, University of Kentucky, Lexington, KY 40536

[2]Center for Pharmaceutical Research and Innovation (CPRI), University of Kentucky, Lexington, KY 40536

[3]Department of Biosciences, Rice University, Houston, TX 77005

[4]Department of Molecular and Cellular Biochemistry, University of Kentucky, Lexington, KY 40536

[5]Department of Plant Pathology, University of Kentucky, Lexington, Kentucky 40546

[6]Department of Chemistry, Markey Cancer Center, Kentucky Center for Structural Biology, University of Kentucky, Lexington, KY 40536

Abstract

This study highlights the biochemical and structural characterization of the L-tryptophan C-6 *C*-prenyltransferase PriB from *Streptomyces* sp. RM-5-8. PriB was found to be uniquely permissive to a diverse array of prenyl donors and acceptors including the antibiotic daptomycin (Cubicin®). This study also highlights two additional PTs (FgaPT2 and CdpNPT) as catalysts for daptomycin prenylation where novel prenylated daptomycins also displayed improved antibacterial activities over the parent drug.

*Corresponding Authors: S.S., shanteri.singh@ou.edu; J.S.T., jsthorson@uky.edu; G.N.P., georgep@rice.edu.
[7]Current address: Department of Chemistry and Biochemistry, University of Oklahoma, Norman, OK 73019

Competing Financial Interests

The authors declare the following competing financial interest(s): J.S.T. is a co-founder of Centrose (Madison, WI)

Author Contributions

S.I.E. and H.C. contributed to the experimental design/execution, and manuscript preparation; K.A.S. and L.V.P. contributed to experimental design/execution; T.S. and H.P.S. contributed experimental reagents and consultation; M.L.F. contributed to experimental design/execution and key consultation; G.N.P. and J.S.T. contributed to the experimental design, project oversight and manuscript preparation; S.S. contributed to the experimental design/execution, project oversight and manuscript preparation.

Additional Information

Supplementary information and chemical compound information is available online at http://www.nature.com/naturechemicalbiology/.

DATA AVAILABILITY

Nucleotide sequence data for *pri* cluster is available under GenBank accession code KT895008. The PriB X-ray crystal structures were deposited at the Protein Database Bank: PriB/L-Trp/dimethylallyl *S*-thiolodiphosphate ternary complex (5INJ), the apo structure (5JXM), and the PriB/pyrophosphate binary complex (5K9M). All other data generated or analyzed during this study are included in this published article (and its supplementary information files) or are available from the corresponding author on reasonable request.

Biocatalysts involved in late stage natural product (NP) tailoring modifications (acylation, alkylation, glycosylation, oxidation) are a centerpiece of a number of successful biocatalytic strategies for non-native modification of complex NP core scaffolds[1–3]. Within this context, microbes from unexplored environments are a rich source for new chemical and biocatalytic diversity[4–7]. Herein we describe the discovery and characterization of PriB, a permissive L-tryptophan (L-Trp) C-6 *C*-prenyltransferase (*C*-PT) from the Appalachian Kentucky coal mine fire-associated *Streptomyces* sp. RM-5-8 isolate[8]. Biochemical and structural studies highlight PriB as a highly proficient and substrate permissive PT and to adopt a substrate-binding orientation distinct from most other indole PTs where the antibiotic Cubicin® (daptomycin, DAP) was noted among the range of unique PriB acceptors. A subsequent comparative study of PriB and other model PTs also revealed the indole C-4 *C*-PT FgaPT2 and reverse C-3 *C*-PT CdpNPT capable of DAP prenylation and, in conjuction with PriB, provided three distinct novel *C*- and *N*-prenylated Trp_1 DAPs, two of which displayed improved antibacterial potency over the parent NP. Cumulatively, this study highlights the discovery and biochemical/structural characterization of a uniquely permissive *C*-PT and, for the first time, extends the demonstrated successful application of L-Trp/indole PTs to include *C*- and *N*-alkylation of complex cyclic peptides.

Streptomyces sp. RM-5-8 was recently reported to produce two distinct metabolite classes that structurally share a rare unsaturated hexuronic acid (Fig. 1a, **2**–**4**)[8]. Whole genome sequencing of *Streptomyces* sp. RM-5-8 led to a draft genome consisting of 259 contigs with a mean size of 36,940 bp and a GC percentage of 72.1% (Supplementary Results, Supplementary Fig. 1). Bioinformatic analysis revealed a single putative PT-encoding gene, designated *priB*, clustered with additional genes spanning a region of 25.3 kb (GenBank accession number KT895008, Supplementary Figs. 1 and 2, Supplementary Table 1) encoding putative functions consistent with the proposed biosynthesis of **2** including a tryptophanase (*priA*), two cytochrome P450s (*priC/D*) and two transglycosylases (*priE/F*). The *priB* gene was predicted to encode a 385 amino acid protein (PriB) that belongs to the $\alpha\beta\beta\alpha$ aromatic PT superfamily (Supplementary Figs. 3 and 4, Supplementary Table 1) with close homology to dimethylallyltryptophan synthases (DMATSs)[9,10]. Based on this analysis a putative biosynthetic pathway for **2** was put forth where PriB would catalyze C-6 *C*-prenylation of L-Trp as an early initiating step (Fig. 1a, Supplementary Fig. 5). To test this hypothesis, *N*-His_6-PriB (herein refered to PriB) was heterologously produced in *E. coli* and purified to homogeneity via Ni^{2+}-affinity chromatography. Analytical scale reactions with L-Trp and dimethylallyl pyrophosphate (DMAPP) led to PriB-dependent quantitative conversion to a new prenylated product based on HPLC-DAD-ESI/MS, consistent with the putative function as a L-Trp *C*-PT or DMATS (Supplementary Fig. 6). Reaction optimization to support scale up and product characterization revealed PriB to display relatively broad metal, temperature and pH tolerance (Supplementary Figs. 7 and 8). Subsequent preparative scale reactions followed by preparative HPLC led to a single prenylated product (80% isolated yield). HR-ESI-MS and 1D- and 2D- ^{1}H- and ^{13}C NMR (Supplementary Fig. 9, Supplementary Table 2) confirmed the product as **1** (Fig. 1a), thereby validating the C-6 *C*-PT function of PriB. Reminiscent of PTs IptA and SAML0654[11,12], substitution of L-Trp with 6-methyl-Trp (Fig. 1b, **5;** a substrate in which the C-6 alkylation site is blocked) in the PriB-catalyzed reaction led to efficient (62% conversion) PriB-catalyzed C-7 prenylation of

the substrate surrogate (Fig. 1b, Supplementary Figs. 9 and 10, Supplementary Table 3), highlighting the potential for substrate-based modulation of PriB regiospecificity. Subsequent determination of PriB steady-state kinetic parameters (L-Trp: k_{cat} = 77.7 ± 1.3 min^{-1}, K_m = 1.1 ± 0.05 μM; DMAPP: k_{cat} = 105.6 ± 7.6 min^{-1}, K_m = 2.0 ± 0.35 μM) implicated PriB as notably proficient among DMATSs for which catalytic parameters have been reported (Supplementary Table 4).

To further probe PriB substrate specificity, a range of potential acceptors (Fig. 1b, Supplementary Fig. 10, Supplementary Table 5) and donors (Fig. 1c, Supplementary Fig. 11, Supplementary Table 6) was evaluated under saturating native donor DMAPP or acceptor L-Trp, respectively. This study highlighted PriB-catalyzed prenylation of Trp analogs, simple indoles, and dihydroxynaphthalenes previously identified as DMATS substrates[9] but also revealed a number of additional acceptors beyond the established scope of DMATSs including: anthranilic acid (**28**); uniquely functionalized naphthalenes (**24**); anthraquinones (**23**); phenazines (**22**); and the drug pindolol (**20**; Visken®). Moreover, this acceptor study revealed PriB as one of the first reported DMATSs to date capable of quantitative conversion of both L- and D-Trp. Reminiscent of the phenolic *O*-PT SirD[13], mono- and di-prenylation of 5-hydroxy-L-Trp was also observed (Fig. 1b, **7**), implicating potential for *O*-alkylation in this example. Unlike most other PTs[9], PriB also displayed a surprising flexibility toward longer prenyl donors including geranyl diphosphate (C_{10}; Fig. 1c, 29), farnesyl diphosphate (C_{15}; Fig. 1c, 30) and geranylgeranyl diphosphate (C_{20}; Fig. 1c, 31). To date, similar donor permissivity has only been reported for the recently characterized indolactam V–specific PTs TleC and MpnD[14]. Based on the observed PriB donor tolerance, a subsequent evaluation of non-native synthetic farnesyl diphosphate donor surrogates (Supplementary Figs. 12 and 13, Supplementary Table 6)[15], revealed PriB turnover with 34 farnesyl diphosphate mimetics including phenoxy-, anilino-, phenylsulfanyl- and benzyl-substituted analogs (Fig. 1c, **32**-**65**, Supplementary Figs. 14 and 15) as the first example for PT-catalyzed utilization of diverse non-native farnesyl diphosphate surrogates. Notably, while both acceptor and, to a lesser extent, donor permissive DMATS members have been reported[9,13,14], this cumulative substrate specificity study clearly implicated PriB as among the most proficient and permissive DMATSs reported to date.

Inspired by the observed PriB permissivity, we sought to assess the potential of this catalyst to utilize more complex structures bearing signature pharmacophores recognized by PriB. The model selected for this assessment was the latest first-in-class NP antibiotic daptomycin (DAP, Cubicin®)[16] that contains both L-Trp- and anthranilate (**28**)-related PriB recognition elements. Analytical scale reactions using DAP and DMAPP revealed the formation of a new product (~11% turnover) consistent with DAP prenylation based on LC-MS (Fig. 2a, Supplementary Fig. 16). Based on this newly observed catalytic capability, similar DAP-based prenylation assays with six other representative PTs (Supplementary Figs. 17 and 18, Supplementary Table 7) revealed both FgaPT2 [an indole C-4 *C*-PT[17]] and CdpNPT [an indole reverse C-3 *C*-PT, originally annotated as a *N*-PT[18]] to also successfully catalyze DAP prenylation [65% and 75% (Supplementary Figs. 19 and 20) conversion, respectively]. Subsequent preparative scale reactions followed by preparative HPLC led to single prenylated products from the PriB- and FgaPT2-catalyzed reactions (6% and 15% isolated

yield, respectively). HR-ESI-MS and 1- and 2D- ^{1}H- and ^{13}C NMR confirmed the PriB-catalyzed product to be the 6-*C*-prenyl-Trp$_1$ DAP (**66**) and the FgaPT2-catalyzed product as the *N*-prenyl-Trp$_1$ DAP (**67;** Fig. 2a, Supplementary Figs. 21–23, Supplementary Table 8, Supplementary Note)]. Interestingly, similar CdpNPT-catalyzed preparative-scale reactions followed by HR-ESI-MS and 1- and 2D- ^{1}H- and ^{13}C NMR characterization revealed an inseparable mixture (Fig. 2a, 54 mg, 70% isolated yield, 1:1 mixture) of **67** and the unusual C-3 reverse prenyl product **68** (a putative pathway is highlighted in Supplementary Fig. 24). Given the distinction between previously reported FgaPT2 and CdpNPT PT regiospecificity and that determined in the context of DAP, the products of preparative scale FgaPT2 and CdpNPT reactions with L-Trp were reevaluated. Consistent with the literature, this analysis confirmed FgaPT2 as a catalyst for L-Trp C-4 prenylation (Supplementary Fig. 25, Supplementary Table 9) and poor turnover of L-Trp by CdpNPT (prohibiting sufficient product for characterization). Subsequent antimicrobial susceptibility studies comparing **66**–**68** to DAP revealed *C*-6′- or *N*-Trp$_1$-prenylation (**66** or **67**, respectively) to invoke a 6–10-fold improvement in antibacterial activity (with no apparent change in general cytotoxicity, Supplementary Table 10) implicating increased lipophilicity as a potential contributor, consistent with previously reported DAP structure activity relationship (SAR) studies[19]. In addition to offering new improved DAP analogs, this discovery conceptually sets the stage for the exploration of additional non-native macromolecular peptide/protein-based targets.

To investigate the structural basis for PriB substrate specificity and catalysis, the X-ray crystal structures of apo-PriB (PDB ID 5JXM), PriB/pyrophosphate binary complex (PDB ID 5K9M), and a PriB/L-Trp/dimethylallyl *S*-thiolodiphosphate ternary complex (PDB ID 5INJ) were determined at 1.15, 1.50 and 1.40 Å resolution, respectively (Supplementary Table 11). Reminiscent of the PT-barrel fold of aromatic and indole PTs[20,21] (Supplementary Fig. 26), PriB is comprised of a central β-barrel, formed by a cylindrical β-sheet arranged around a solvent-filled core surrounded by a ring of solvent-exposed α-helices. A comparison of apo-PriB to that of ligand bound structures revealed substantial side chain rearrangement (most notably, 123° and 34° rotation of Arg108 and Tyr181, respectively) within the active site and loop regions around the active site upon substrate binding mediated via both key hydrophobic and hydrogen bonding interactions (Supplementary Fig. 27). Consistent with a lack of divalent metal influence on PriB catalysis, the side chain amines of PriB Arg108 and Lys179 in substrate-bound PriB occupy the divalent cation-binding site of corresponding metal dependent PTs (Fig. 2b)[20]. PriB substrate orientation in ligand-bound structures is most similar to that of indole C-7-PTs (MpnD and TleC, both enzymes displaying broad donor specificity)[14] and clearly distinct to that of the corresponding C-2- (FtmPT1), C-4- (FgaPT2) or C-3-PTs (CdpNPT) (Supplementary Fig. 28) with the DMSPP C-1 located within the 3.6 Å of the indole C-6 or C-7 (Supplementary Fig. 27). The unique substrate orientation within PriB and/or the observed PriB binding pocket dynamics upon substrate binding are potential contributors to the catalyst's expanded permissivity. Similar to other indole PTs[22], conserved aromatic residues (Tyr181, Tyr236 and Tyr380) stabilize the prenyl carbocation via π-cation interactions and a conserved glutamic acid (Glu94) is poised as a general base for indole activation where the PriB His312 imidazole may further stabilize indole C-6 transition-state

charge density (Supplementary Fig. 27). Interestingly, this latter histidine is also conserved in the indole C-6-PTs SAML0654 and Strvi8510[13] (Supplementary Fig. 26).

In summary, genome mining of an Appalachian underground coal mine fire-associated microbe enabled the discovery and characterization of the L-Trp C-6 *C*-PT postulated to play a key role in **2** biosynthesis. The observed enhanced proficiency and expanded donor/acceptor substrate permissivity of PriB is consistent with similar proficiency/permissivity correlations observed among other native or engineered enzymes[23,24]. As a biocatalyst, PriB is robust and catalyzes a reaction (indole C-6 alkylation) that remains a challenge to conventional synthetic strategies[25] where the permissiveness of PriB (and other PTs) enables complementary synthetic strategies that might be further enhanced via structure-based engineering.

ONLINE METHODS

Strains and materials

Streptomyces sp. RM-5-8 was isolated from the Ruth Mullins underground coal mine fire site and was provided by the University of Kentucky CPRI Natural Products Repository. All primers were purchased from Integrated DNA Technology, *E. coli* 5α and BL21(DE3) competent cells were purchased from New England Biolabs. Dimethylallyl S-thiolodiphosphate (DMSPP) was purchased from Echelon Biosciences. Polyethylene glycol 3350 (PEG 3350) and PEG 4000 both in the form of a 50% w/v solution, as well as crystallization screens Index HT, PEGRx HT, Crystal Screen HT and SaltRx HT were obtained from Hampton Research. Crystallization screens JCSG-plus HT-96, Morpheus and MIDAS were from Molecular Dimensions. All other reagents and chemicals were purchased from Sigma-Aldrich or Fisher Scientific and were used without further purification unless otherwise stated. PD-10 columns and Ni-NTA superflow columns were purchased from GE Healthcare. All non-native synthetic prenyl donors were synthesized as previously reported[26,27]. All solvents used were of ACS grade and purchased from Pharmco-AAPER. All DNA sequencing was conducted with the primers T7 promoter (5′-TAATACGACTCACTATAGGG-3′) and T7 terminator (5′-GCTAGTTATTGCTCAGCGG-3′). Daptomycin (DAP, Cubicin®) was generously provided by Merck.

General methods

NMR spectra were obtained at ambient temperature on Varian Unity Inova 400, 500 or 600 MHz instruments (University of Kentucky College of Pharmacy NMR facility) using 99.8% d_6-DMSO (Cambridge Isotope Laboratories), as a solvent. Chemical shifts were referenced to internal solvent resonances and are reported in parts per million (ppm) with coupling constants J given in Hz. Analytical TLC was performed on silica gel glass TLC plates (EMD Millipore). Visualization was accomplished with UV light (254 nm) followed by staining with vanillin-sulfuric acid reagent and heating. HPLC was accomplished on an Agilent 1260 HPLC system equipped with a DAD detector (Methods A, B, and C), a Waters 2695 separation module equipped with a Waters 2996 photodiode array detector and a Waters Micromass ZQ (Methods D and E), or a Varian Prostar 210 HPLC system equipped with a

photodiode array detector (Methods F and G) HPLC peak areas were integrated with Varian Star Chromatography Workstation Software and the percent conversion calculated as a percent of the total peak area. High resolution electrospray ionization (ESI) mass spectra were recorded on an Exactive Orbitrap mass spectrometer (Thermo Scientific).

HPLC Method A—Luna C-18 (5μm, 4.6 mm × 250 mm) column (Phenomenex) [10% B for 5 min, gradient of 10% B to 100% B over 18 min, 100% B for 5 min, 100% B to 10% B over 1 min, 10% B for 4 min (A = ddH_2O with 0.1% formic acid; B = acetonitrile) flow rate = 1 mL min^{-1}; A_{280}].

HPLC Method B—Luna C-18 (5μm, 4.6 mm × 250 mm) column (Phenomenex) [20% B for 5 min, gradient of 20% B to 100% B over 16 min, 100% B for 7 min, 100% B to 20% B over 1 min, 20% B for 4 min (A = ddH_2O with 0.1% formic acid; B = acetonitrile) flow rate = 1 mL min^{-1}; A_{280}].

HPLC Method C—Luna C-18 (5μm, 4.6 mm × 250 mm) column (Phenomenex) [10% B for 5 min, gradient of 10% B to 100% B over 10 min, 100% B for 13 min, 100% B to 10% B over 1 min, 10% B for 4 min (A = ddH_2O with 0.1% formic acid; B = acetonitrile) flow rate = 1 mL min^{-1}; A_{280}].

HPLC Method D—Kinetex EVO C-18 (5μm, 4.6 mm × 250 mm) column (Phenomenex) [10% B for 5 min, gradient of 10% B to 100% B over 21 min, 100% B for 4 min, 100% B to 10% B over 1 min, 10% B for 4 min (A = ddH_2O with 0.1% formic acid; B = acetonitrile with 0.1% formic acid) flow rate = 0.5 mL min^{-1}; A_{280}].

HPLC Method E—Kinetex EVO C-18 (5μm, 4.6 mm × 250 mm) column (Phenomenex) [10% B for 5 min, gradient of 10% B to 100% B over 15 min, 100% B for 10 min, 100% B to 10% B over 1 min, 10% B for 4 min (A = ddH_2O with 0.1% formic acid; B = acetonitrile with 0.1% formic acid) flow rate = 0.5 mL min^{-1}; A_{280}].

HPLC Method F—Supelco Discovery® Bio wide pore C-18 (10 μm, 250 × 21.2 mm) column (Sigma-Aldrich) [10% B for 5 min, gradient of 10% B to 100% B over 15 min, 100% B for 10 min, 100% B to 10% B over 1 min, 10% B for 4 min (A = ddH_2O with 0.05% formic acid; B = acetonitrile) flow rate = 8 mL min^{-1}; A_{280}].

HPLC Method G—Gemini C-18 (5 μm, 10 × 250 mm) column (Phenomenex) [10% B for 2 min, gradient of 10% B to 100% B over 13 min, 100% B for 3 min, 100% B to 10% B for 4 min, 10% B for 4 min (A = ddH_2O with 0.1% Trifluoroacetic acid; B = acetonitrile) flow rate: 5.0 mL min^{-1}; A_{280}].

DNA extraction, genome sequencing and analyses

Streptomyces sp. RM-5-8 was grown on M2-medium agar (glucose, 4.0 g L^{-1}; Bacto yeast extract, 4.5 g L^{-1}; Bacto malt extract, 10 g L^{-1}; calcium carbonate, 2.0 g L^{-1}; agar, 17.0 g L^{-1}) for four days at 28°C. Pure colonies were used to inoculate a 250 mL Erlenmeyer flask containing 50 mL of liquid medium A (soluble starch, 20.0 g L^{-1}; glucose, 10.0 g L^{-1}; Bacto peptone, 5.0 g L^{-1}; Bacto yeast extract, 5.0 g L^{-1}; NaCl, 4.0 g L^{-1}; K_2HPO_4, 0.5 g

L^{-1}; $MgSO_4 \cdot 7H_2O$, 0.5 g L^{-1}; $CaCO_3$, 2.0 g L^{-1}). After three days of incubation at 28°C with 200 rpm agitation, the cell pellet was collected by centrifugation at 5,000 ×*g* for 15 min. Genomic DNA was extracted using an UltraClean Microbial DNA Isolation Kit (MoBio laboratories, Inc) following manufacturer's protocol. DNA quality and concentration were assessed using gel electrophoresis and Nanodrop 2000c spectrophotometer (Thermo Scientific) and purity was confirmed using 16S rRNA analysis. The resultant DNA solution was subjected to massively parallel sequencing using Miseq sequencer (Illumina) at the University of Kentucky Advanced Genetic Technologies Center (UK-AGTC). The genome (10.5 Mb, 28× coverage) was assembled using Newbler v.2.9 (Roche Diagnostics). Low quality regions were sequence verified by polymerase chain reaction and Sanger sequencing. Putative prenyltransferase (PT) genes were identified via Basic Local Alignment Search Tool (BLAST) comparison of the final assembly to a group of 52 fungal and bacterial PT genes (Supplementary Fig. 3). Homology searches of the generated contigs were carried out using the BLASTX and Position-Specific Iterated BLAST (PSI-BLAST). Gene alignments and analyses were performed using Geneious Pro 5.0.3[28] (Supplementary Table 1 and Supplementary Fig. 5). The sequence of the putative *pri* biosynthetic gene cluster of **2** has been deposited under GenBank accession number KT895008.

Gene cloning and protein production and purification

The *priB* gene was amplified from *Streptomyces sp.* RM-5-8 genomic DNA using the primers PriB-NdeI-F AGGCCATATGGGAGGTCCGATGAGCGGTTTCCA and PriB-HindIII-R TATTAAGCTTTCACAGCCGTGCCCGCGCCCGGTC (engineered restriction sites underlined). The corresponding fragment was cloned into the *E. coli* expression vector pET28a (Novagen) and confirmed via sequencing. The validated expression plasmid (pSEPriB) was subsequently transformed into *E. coli* BL21 (DE3) competent cells (New England Biolabs). Production strains for the group of previously reported fungal and bacterial PTs were constructed in a similar fashion from synthetic genes (GenScript); Supplementary Table 8). All studies employed the corresponding *N*-terminal-His_6 fusion proteins.

For protein production, 1L of LB broth (Becton, Dickinson and Company) supplemented with kanamycin (50 μg mL^{-1}) was inoculated with 0.1% (v/v) of an overnight pSEPriB-*E. coli* BL21 (DE3) seed culture and grown at 37°C with shaking (225 rpm). Cultures were induced at OD_{600} of ~0.6–0.8 with isopropyl-β-D-thiogalactopyranoside (IPTG, 0.5 mM final concentration) and allowed to grow for an additional 16 hr at 22°C. Cells were harvested by centrifugation and stored in lysis buffer (10 mM imidazole, 50 mM sodium monobasic phosphate, 300 mM NaCl, pH 8.0) at −80°C until used. All subsequent steps were carried out on ice. Cells were allowed to thaw and were subsequently lysed by sonication (Virtis VirSonic 475 with a microtip, 100W, 10 × 10 sec pulses, 20 sec between pulses). Insoluble debris was removed by centrifugation at 15,000 ×*g* for 1 hr. The supernatant was collected and filtered using 0.22 μm filters and the desired *N*-His_6-PriB fusion protein was purified via HiTrap nickel-nitrilotriacetic acid (Ni-NTA) affinity chromatography using standard protocols with AKTA Purifier 10 (GE Healthcare). Buffer exchange of each sample was performed using a PD-10 column (GE Healthcare) eluted with

50 mM Tris, 100 mM NaCl, pH 8.0 to yield 5 mg L^{-1} PriB. Fractions were collected and concentrated using Amicon Ultra Centrifuge columns 30,000 MWCO (EMD Millipore) and stored in 50 mM Tris, 100 mM NaCl, pH 8.0 at −80°C. Protein concentrations were determined by Bradford assay (BioRad) using bovine serum albumin as a standard. Purity and presence of proteins were confirmed by SDS-PAGE gel electrophoresis. The *N*-His_6-PriB fusion protein (referred to as PriB) was used for all studies. Production of other PTs for the overall study (Supplementary Table 8) followed the same protocol.

Analytical assays and enzyme kinetics

Standard PriB *in vitro* assays were conducted in 1.5 mL tubes in a volume of 100 μL Tris 50 mM (pH 8.0) containing a final concentration of 0.5 mM L-Trp, 1 mM DMAPP, and 250 nM PriB. After preincubation of the reaction mixture at 37°C for 10 min, the reactions were initiated by the addition of enzyme and allowed to proceed for 60 min (unless otherwise noted) at 37°C. The reactions were quenched by the addition of 100 μL MeOH and mixing followed by centrifugation (22,000 ×*g*, 15 min, 4°C) to remove precipitated protein. The supernatants were analyzed by HPLC using *Method A* (see General methods) to calculate conversion rate based on the area of substrate and the prenylated product peaks. Where applicable, subsequent product mass analyses (Supplementary Tables 5 and 6, Supplementary Note) were typically accomplished via direct LC-MS (LC-ESI-MS, *Method D* or *E*, see General Methods) and/or HR-ESI-MS of HPLC-purified products (*Method A*).

Temperature optimization—Replicates of the standard assay were conducted at 4, 10, 20, 30, 37, 45, 55, 65°C.

pH optimization—Replicates of the standard assay were modified via substitution of Tris 50 mM (pH 8.0) with 50 mM citric acid-sodium dihydrogen phosphate (pH 3.5–8.0) or 50 mM glycine-sodium hydroxide (pH 8.5–11.0).

Various cation assessment—Replicates of the standard assay were conducted in the presence of 5 or 10 mM of each of the following: EDTA, $MgCl_2$, $CuCl_2$, $MnCl_2$, LiCl, $BaCl_2$, $CoCl_2$, $CaCl_2$, $ZnCl_2$, and $SrCl_2$.

Determination of kinetic parameters—Replicates of the standard assay were used with variable acceptor ([L-Trp] = $1x10^{-3}$–5 mM) and fixed donor ([DMAPP] = 1 mM) or variable donor ([DMAPP] = 0.5–4 mM) and fixed acceptor ([L-Trp] = 0.5 mM) in triplicate. The kinetic constants were calculated by nonlinear regression fit to the Michaelis-Menten equation using GraphPad Prism 7 software.

PriB substrate specificity—Replicate assays were performed with 0.5 mM acceptor and 0.3–2 mM donor in the presence of 2 μM purified PriB in 50 mM Tris pH 8.0 for 16 hr.

Daptomycin catalyst survey—Replicates assays contained 1 μM enzyme, 1 mM DAP, and 1 mM DMAPP in the presence of 50 mM Tris (pH 8.0). Assays containing FgaPT2 or CdpNPT were supplemented with 10 mM $CaCl_2$.

Prenylated L-Trp product isolation/characterization

For isolation and full characterization of prenylated Trp analogs, 0.5 mL reactions (×20) in 1.5 mL Eppendorf tubes containing 2.5 mM acceptor (L-Trp or 6-methyl-DL-Trp), 2.5 mM DMAPP, 5 μM enzyme (PriB or FgaPT2) in 50 mM Tris (pH 8.0) were incubated for 16 hr at 37°C. Divalent cation (10 mM $CaCl_2$) was also included in all FgaPT2-catalyzed reactions. Reactions were combined, terminated by mixing with equal volume of MeOH, centrifuged to remove precipitated protein and dried under reduced pressure. The crude reaction mixture was redissolved in MeOH and purified via preparative HPLC (*Method F*).

4-dimethylallyl-L-Trp (70)—White solid (5.6 mg, 56% isolation yield); (+)-ESI-MS: *m/z* 273 $[M + H]^+$; (+)-HR-ESI-MS: *m/z* 273.1596 $[M + H]^+$ (calcd for $C_{16}H_{20}N_2O_2$, 273.1598). ^1H NMR (d_6-DMSO, 400 MHz) and ^{13}C NMR (d_6-DMSO, 100 MHz); see Supplementary Fig. 25, Supplementary Table 9, Supplementary Note.

6-dimethylallyl-L-Trp (1)—White solid (8 mg, 80% isolation yield); (+)-ESI-MS: *m/z* 273 $[M + H]^+$; (+)-HR-ESI-MS: *m/z* 273.1598 $[M + H]^+$ (calcd for $C_{16}H_{20}N_2O_2$, 273.1598). ^1H NMR (d_6-DMSO, 400 MHz) and ^{13}C NMR (d_6-DMSO, 100 MHz); see Supplementary Fig. 9, Supplementary Table 2, Supplementary Note.

6-methyl-7-dimethylallyl-L-Trp (69)—White solid (6 mg, 15% isolation yield); (+)-ESI-MS: *m/z* 287 $[M + H]^+$; (+)-HR-ESI-MS: *m/z* 287.1753 $[M + H]^+$ (calcd for $C_{17}H_{23}N_2O_2$, 287.1754). ^1H NMR (d_6-DMSO, 400 MHz) and ^{13}C NMR (d_6-DMSO, 100 MHz); see Supplementary Fig. 9, Supplementary Table 3, Supplementary Note.

Prenylated DAP product isolation/characterization

For isolation and full characterization of prenylated DAP analogs, reactions containing 1 mM DAP, 1 mM DMAPP and 1 μM enzyme (PriB, FgaPT2 or CdpNPT) in 50 μL Tris (pH 8.0) were incubated for 12 hr at 37°C. FgaPT2 and CdpNPT-catalyzed reactions also contained divalent cation (10 mM $CaCl_2$). Reactions were terminated by mixing with equal volume of MeOH, centrifuged to remove precipitated protein and dried under reduced pressure. Crude reaction mixtures were subsequently redissolved in MeOH and purified via preparative HPLC (*Method G*).

6′-C-prenyl-Trp$_1$ DAP (66)—White solid (0.6 mg, 6% isolation yield); (−)-ESI-MS: *m/z* 1687 $[M - H]^-$; (−)-HR-ESI-MS: *m/z* 1686.7635 $[M - H]^-$ (calcd for $C_{77}H_{108}N_{17}O_{26}$, 1686.7657). ^1H NMR (d_6-DMSO, 600 MHz) and ^{13}C NMR (d_6-DMSO, 150 MHz); see Supplementary Figs. 21–23, Supplementary Table 8, Supplementary Note.

N-prenyl-Trp$_1$ DAP (67)—White solid (6 mg, 60% isolation yield); (−)-ESI-MS: *m/z* 1687 $[M - H]^-$; (−)-HR-ESI-MS: *m/z* 1686.7603 $[M - H]^-$ (calcd for $C_{77}H_{108}N_{17}O_{26}$, 1686.7657); (+)-HR-ESI-MS: *m/z* 1688.7870 $[M + H]^+$ (calcd for $C_{77}H_{110}N_{17}O_{26}$, 1688.7802); ^1H NMR (d_6-DMSO, 400 MHz) and ^{13}C NMR (d_6-DMSO, 100 MHz); see Supplementary Figs. 21–23, Supplementary Table 8, Supplementary Note.

CdpNPT prenylated daptomycin mixture (67/68)—White solid (53 mg, 70% isolation yield, mixture 1:1); (−)-ESI-MS: *m/z* 1687 $[M - H]^-$; (−)-HR-ESI-MS: *m/z* 1686.7655 $[M - H]^-$ and $[(M - H_2O) - H]^-$ (calcd for $C_{77}H_{108}N_{17}O_{26}$, 1686.7657); ^1H NMR (d_6-DMSO, 400 MHz) and ^{13}C NMR (d_6-DMSO, 100 MHz); see Supplementary Figs. 21–23, Supplementary Table 8, Supplementary Note.

Bioactivity assays

All DAP and DAP analog stocks were calibrated by absorbance (ε_{366} = 4,000 L mol^{-1} cm^{-1})[29] and all bioactivity assays were conducted in triplicate. Antimicrobial activities were determined following a previously reported protocol[30]. Strain growth also followed our prior protocol[11] where LB medium (BD244620) was used for *B. subtilis* and Middlebrook 7H9 with OADC enrichment (Sigma-Aldrich) for *M. aurum*. Cancer cell-line cytotoxicity assays as a measure of general eukaryotic cell toxicity employed the human lung non-small-cell carcinoma cell line A549 as previously reported[30].

Crystallization, diffraction data collection, and structure determination of PriB

PriB from Ni-affinity chromatography was further purified via gel filtration (Superdex 200; 50 mM Tris pH 7.5 buffer, 100 mM NaCl) via an AKTAprime Plus FPLC system (GE Healthcare), concentrated with Amicon® Ultra-4 Centrifugal Filter Units (EMD Millipore) to final concentration of 34 mg mL^{-1}, drop flash-frozen and stored at −80°C prior to use. Initial crystallization trials were set up by mosquito® Crystal nanoliter dispenser robot (TTP Labtech) on MRC 2 Well crystallization plates (Hampton Research) using sitting drop vapor diffusion method testing against all seven commercial high-throughput screens each with 96 conditions. PriB was crystallized by sitting drop vapor diffusion using a 1:1 v/v mixing of 10 mg mL^{-1} PriB solution in the presence of 1 mM L-Trp with reservoir solution containing 0.1 M Tris, pH 8.5, 20% w/v PEG 3350, 0.1 M $MgCl_2$. The mixed drops of 0.4–1 μL were equilibrated over a reservoir solution of 50 μL and incubated at 20°C in the dark. Monoclinic shaped crystals grew after 6–10 days with the longest dimension typically reaching 100–600 μm. The iodine derivative was prepared by soaking a solution of 0.5 M sodium iodide, 50 mM Tris pH 8.5, 10% w/v PEG 3350, 0.05 M $MgCl_2$ into a drop of PriB crystals (grown under the same condition as the apo form) at a 1:3 v/v mixing ratio. The ternary complex was obtained by soaking a solution of 25 mM substrate mimic dimethylallyl *S*-thiolodiphosphate (DMSPP), 50 mM Tris, pH 8.5, 10% w/v PEG 3350, 0.05 M $MgCl_2$ into PriB crystals (grown under conditions similar to the native form in the presence of substrate 1 mM L-Trp at pH 8.0) at a 1:1.5 v/v mixing ratio. The product diphosphate bound form was obtained by growing PriB crystals using the same sitting drop procedure but under different conditions by 1:1 v/v mixing of 10 mg mL^{-1} PriB solution in the presence of 1 mM dimethylallyl diphosphate (DMAPP) with reservoir conditions containing 100 mM Tris, pH 8.0, 28% w/v PEG 4000. Crystals of the native form and ternary complex were cryoprotected by transferring into MiTeGen's LV CryoOil (MiTeGen) and flash-frozen in liquid nitrogen. The crystal of the diphosphate complex was directly flash-frozen in liquid nitrogen without additional cryoprotectant.

Diffraction data were collected at the Advanced Photon Source at Argonne National Laboratory on the LRL-CAT (31-ID-D) beamline. The detector used was a Rayonix 225 HE

CCD (Rayonix) using a single wavelength of 1.3776 Å for the iodine derivative and 0.97931 Å for all other datasets. The anomalous dataset was collected and processed to a resolution of 1.54 Å, the apo form to 1.15 Å, the ternary complex to 1.4 Å, and the diphosphate complex to 1.5 Å (Supplementary Table 11). The anomalous and apo datasets were indexed, integrated, and scaled using XDS[31]. The substrate/product complexes datasets were indexed and integrated by MOSFLM, scaled and merged by SCALA from the CCP4 program suites[32]. The structure of PriB was determined by single-wavelength anomalous diffraction (SAD) phasing on the iodine derivative dataset using AutoSol from the PHENIX software suite[33]. One copy of the polypeptide was found and built in the asymmetric unit with 26 iodine atoms of various occupancy. The sparsity of intermolecular contacts (largest interface area < 530 $Å^2$) in the crystal packing suggest the protein is a monomer. Analysis of crystal contact suggests the protein to be a monomer. The protein model as traced from the iodide containing dataset was then used as the search model for solving the apo and ligand complexes by molecular replacement with Phaser_MR and Autobuild of the PHENIX suite[33]. Most of the amino acid residues were successfully built with traceable electron density except for short stretches at the N and C termini, as well as one short flexible loop away from the active site. Ligands and alternative conformations of residues were built into the model based on difference electron density maps. The structures were completed with alternating rounds of manual model building with COOT[34] and refinement with PHENIX. Water was added and updated during refinement. The final structures were refined to the same resolution limits as in data collection with favorable R_{cryst} and R_{free} values (Supplementary Table 11). Model quality was assessed using MolProbity[35]. Ramachandran statistics determined as the percentage of residues were 98.9, 1.1, 0.0 in the most favored, additionally allowed and outlier regions of the Ramachandran diagram, respectively. All structures were rendered using PyMOL[35].

Supplementary Material

Refer to Web version on PubMed Central for supplementary material.

Acknowledgments

This work was supported by NIH grants R37 AI52188 and R01 CA203257 (JST), U01 GM098248 (GNP) and NCATS (UL1TR001998). Daptomycin (Cubicin®) was generously provided by Merck. We are grateful to Professors Jürgen Rohr, Steven Van Lanen and Joseph Chappell (College of Pharmacy, University of Kentucky) for helpful discussion and facilitating access to shared equipment and/or reagents. We thank the University of Kentucky Mass Spectrometry Facility for the HR-ESI-MS support. This research also used resources of the Advanced Photon Source, a U.S. Department of Energy (DOE) Office of Science user facility operated by Argonne National Laboratory (DE-AC02-06CH11357). Use of the Lilly Research Laboratories Collaborative Access Team (LRL-CAT) beamline at Sector 31 of the Advanced Photon Source was provided by Eli Lilly Company.

References

1. Walsh CT. Nat Chem Biol. 2015; 11:620–624. [PubMed: 26284660]
2. Tibrewal N, Tang Y. Annu Rev Chem Biomol Eng. 2014; 5:347–366. [PubMed: 24910918]
3. Gantt RW, Peltier-Pain P, Thorson JS. Nat Prod Rep. 2011; 28:1811–1853. [PubMed: 21901218]
4. Elshahawi SI, et al. Proc Natl Acad Sci U S A. 2013; 110:E295–304. [PubMed: 23288898]
5. Ling LL, et al. Nature. 2015; 517:455–459. [PubMed: 25561178]
6. Donia MS, Fischbach MA. Science. 2015; 349:1254766. [PubMed: 26206939]

7. Carr G, et al. Org Lett. 2012; 14:2822–2825. [PubMed: 22591554]
8. Wang X, et al. Org Lett. 2015; 17:2796–2799. [PubMed: 25961722]
9. Fan A, Winkelblech J, Li SM. Appl Microbiol Biotechnol. 2015; 99:7399–7415. [PubMed: 26227408]
10. Rudolf JD, Wang H, Poulter CD. J Am Chem Soc. 2013; 135:1895–1902. [PubMed: 23301871]
11. Takahashi S, et al. J Bacteriol. 2010; 192:2839–2851. [PubMed: 20348259]
12. Winkelblech J, Li SM. Chembiochem Eur J Chem Biol. 2014; 15:1030–1039.
13. Rudolf JD, Poulter CD. ACS Chem Biol. 2013; 8:2707–2714. [PubMed: 24083562]
14. Mori T, et al. Nat Commun. 2016; 7:10849. [PubMed: 26952246]
15. Subramanian T, Liu S, Troutman JM, Andres DA, Spielmann HP. Chembiochem Eur J Chem Biol. 2008; 9:2872–2882.
16. Eisenstein BI, Oleson FB, Baltz RH. Clin Infect Dis Off Publ Infect Dis Soc Am. 2010; 50(Suppl 1):S10–15.
17. Unsöld IA, Li SM. Microbiol Read Engl. 2005; 151:1499–1505.
18. Mahmoodi N, Tanner ME. ChemBioChem. 2013; 14:2029–2037. [PubMed: 24014462]
19. Yin N, et al. J Med Chem. 2015; 58:5137–5142. [PubMed: 25993059]
20. Kuzuyama T, Noel JP, Richard SB. Nature. 2005; 435:983–987. [PubMed: 15959519]
21. Bonitz T, Alva V, Saleh O, Lupas AN, Heide L. PloS One. 2011; 6:e27336. [PubMed: 22140437]
22. Tanner ME. Nat Prod Rep. 2015; 32:88–101. [PubMed: 25270661]
23. Williams GJ, Zhang C, Thorson JS. Nat Chem Biol. 2007; 3:657–662. [PubMed: 17828251]
24. Nobeli I, Favia AD, Thornton JM. Nat Biotechnol. 2009; 27:157–167. [PubMed: 19204698]
25. Feng Y, et al. J Am Chem Soc. 2015; 137:10160–10163. [PubMed: 26256033]
26. Chehade KAH, et al. J Am Chem Soc. 2002; 124:8206–8219. [PubMed: 12105898]
27. Subramanian T, Wang Z, Troutman JM, Andres DA, Spielmann HP. Org Lett. 2005; 7:2109–2112. [PubMed: 15901146]
28. Kearse M, et al. Bioinforma Oxf Engl. 2012; 28:1647–1649.
29. Debono M, et al. J Antibiot (Tokyo). 1988; 41:1093–1105. [PubMed: 2844711]
30. Shaaban KA, et al. J Nat Prod. 2015; 78:1723–1729. [PubMed: 26091285]
31. Kabsch W. Acta Crystallogr D Biol Crystallogr. 2010; 66:125–132. [PubMed: 20124692]
32. Collaborative Computational Project, Number 4. Acta Crystallogr D Biol Crystallogr. 1994; 50:760–763. [PubMed: 15299374]
33. Adams PD, et al. Acta Crystallogr D Biol Crystallogr. 2010; 66:213–221. [PubMed: 20124702]
34. Emsley P, Lohkamp B, Scott WG, Cowtan K. Acta Crystallogr D Biol Crystallogr. 2010; 66:486–501. [PubMed: 20383002]
35. Chen VB, et al. Acta Crystallogr D Biol Crystallogr. 2010; 66:12–21. [PubMed: 20057044]

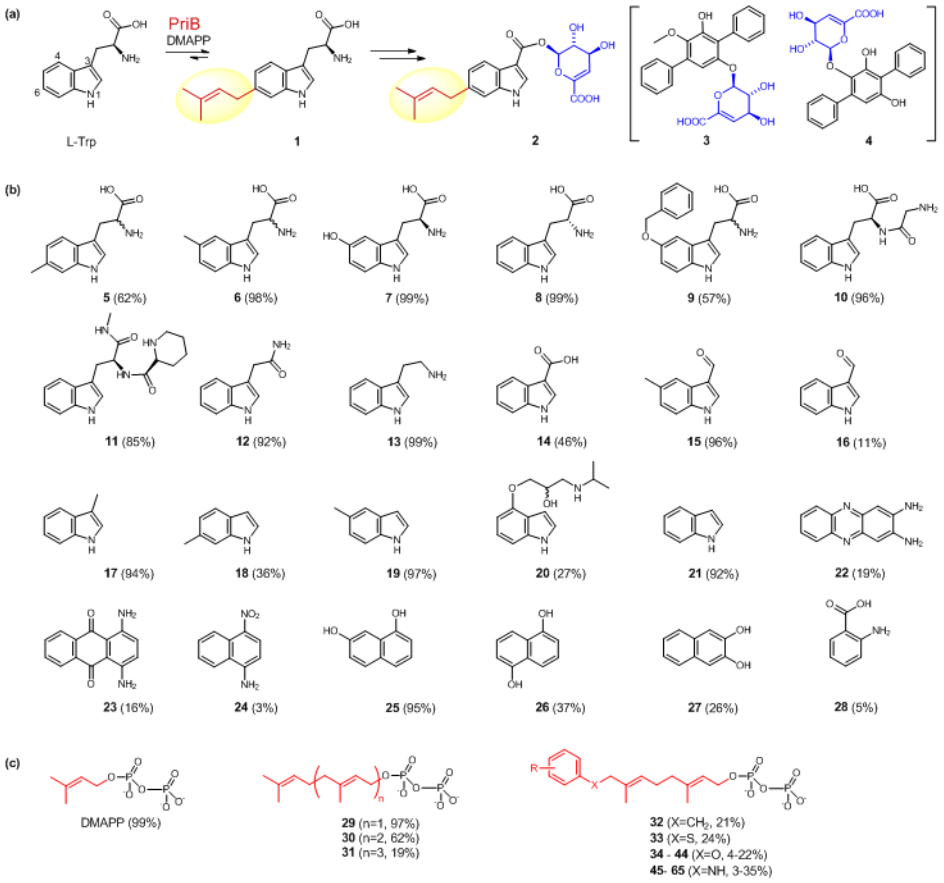

Fig. 1. PriB discovery and permissiveness of PriB and other indole PTs

(a) Genome mining revealed the putative locus for the biosynthesis of **2**, including PriB. **(b, c)** Substrate permissivity of PriB. Percent conversion (in parentheses) of enzyme reactions containing constant native donor (DMAPP) and variable prenyl acceptors (**5**–**28**) for **(b)** or constant native acceptor (L-Trp) and variable donors (**29**–**65**) for **(c)** (n=2; see also Supplementary Figs. 12 and 13 and Supplementary Tables 5 and 6).

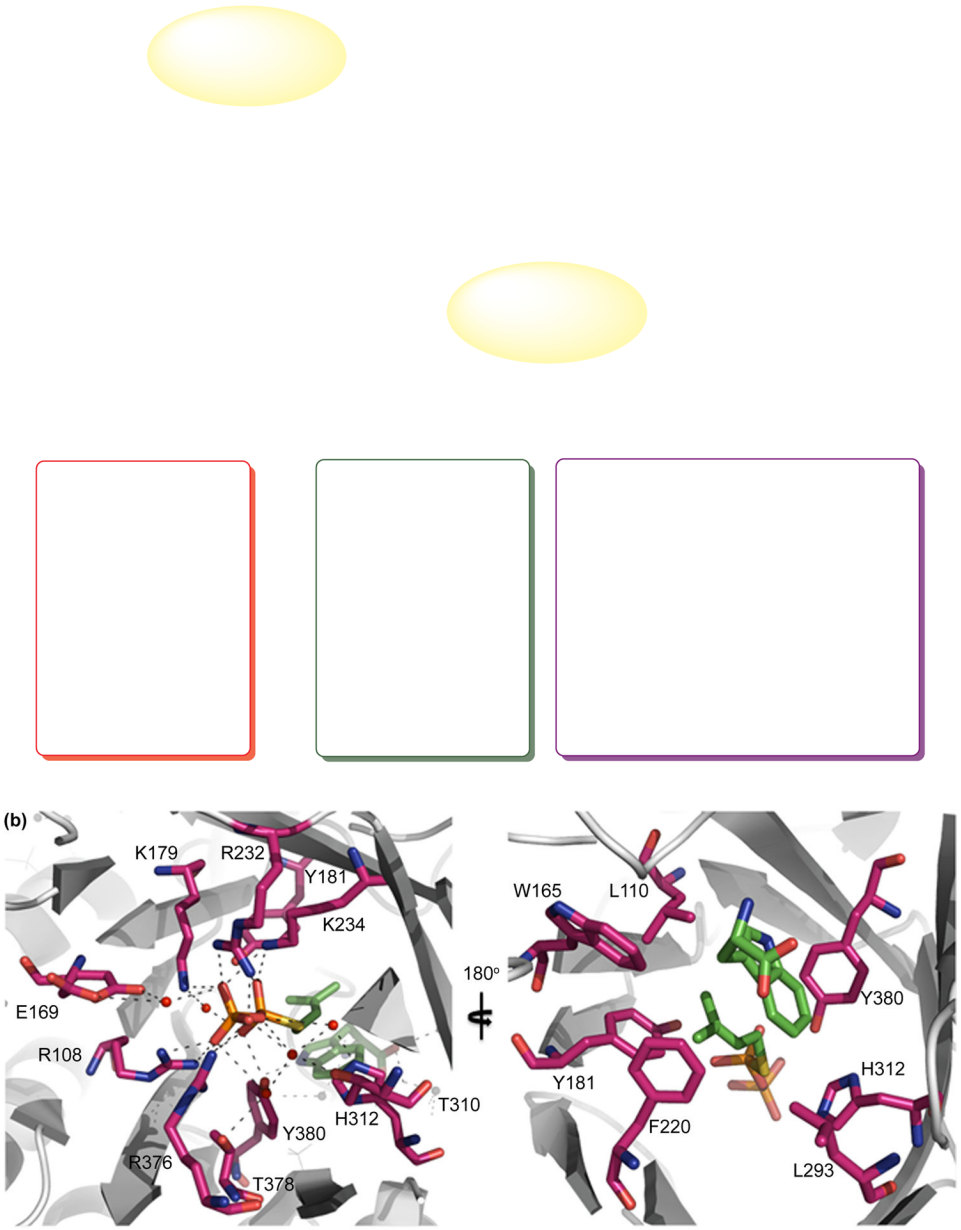

Fig. 2. Prenylated daptomycins (DAPs) and the crystal structure of PriB

(**a**) Products of PriB-, FgaPT2- and CdpNPT-catalyzed prenylation of DAP. (**b**) PriB active site residues and corresponding ligand hydrogen bond interactions (left, front and right, back perspective). The ligands are illustrated as ball-and-stick models, with the following color code: carbon, green; oxygen, red; nitrogen, blue; phosphorous, orange; sulfur, yellow; water, red spheres; and putative hydrogen-bonding interations, dashed brown lines.